Synergistic Design of Molten Salt-Exfoliated CuS/C_3N_4 Heterojunction: Elucidating Photogenerated Charge Transfer Behavior and Mechanism for Enhanced Photocatalytic Hydrogen Evolution

Xiaobo Liang[a], Chunhai Qi[a], Lingdan Dong[a], Chunyi Xu[b], Wenhao Zhang[b], Lingling Bi*[b], Wei Jiang[a]

[a] Jiangsu Key Laboratory of Advanced Manufacturing Technology, Faculty of Mechanical and Material Engineering, Huaiyin Institute of Technology, Huai'an, 223003, People's Republic of China.

[b] College of Chemical Engineering, Key Laboratory for Palygorskite Science and Applied Technology of Jiangsu Province, National & Local Joint Engineering Research Center for Mineral Salt Deep Utilization, Huaiyin Institute of Technology, Huai'an, 223003, People's Republic of China.

* Corresponding author: Lingling Bi

E-mail: jghx8888@hyit.edu.cn

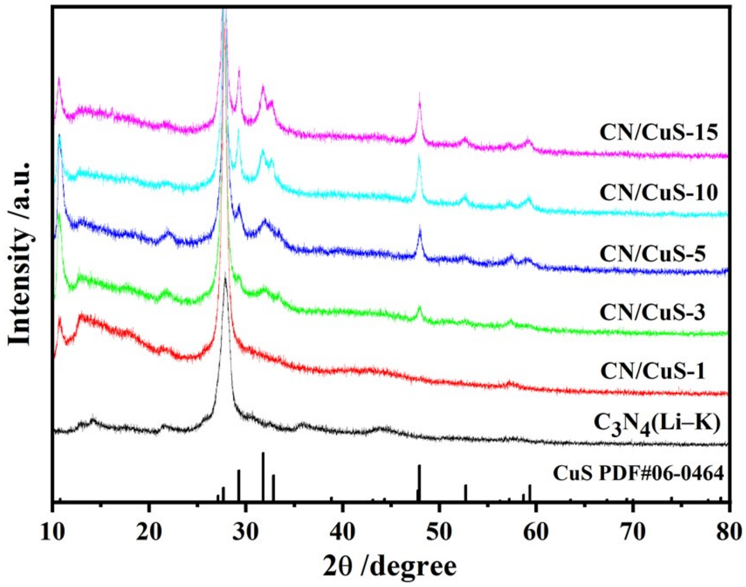

Fig. S1 The enlarged XRD patterns of CuS/C_3N_4(Li–K) photocatalysts.

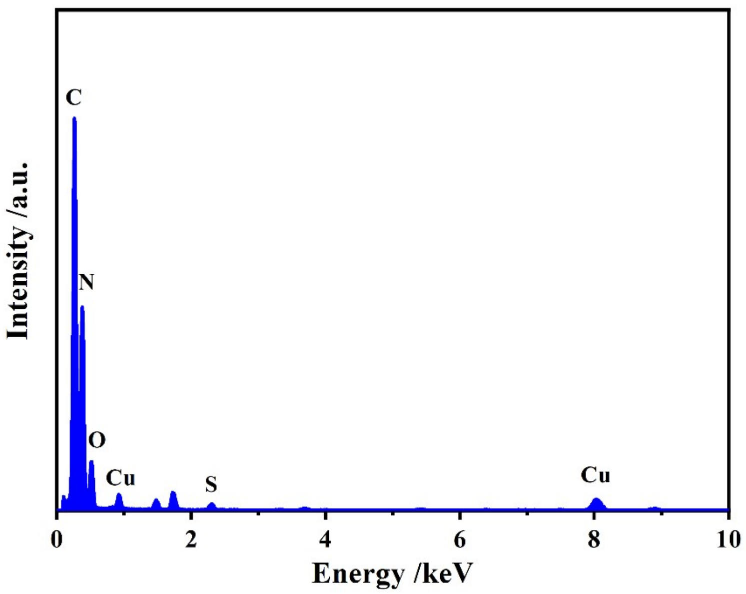

Fig. S2 HRTEM image corresponding EDS images of CN/CuS-3.

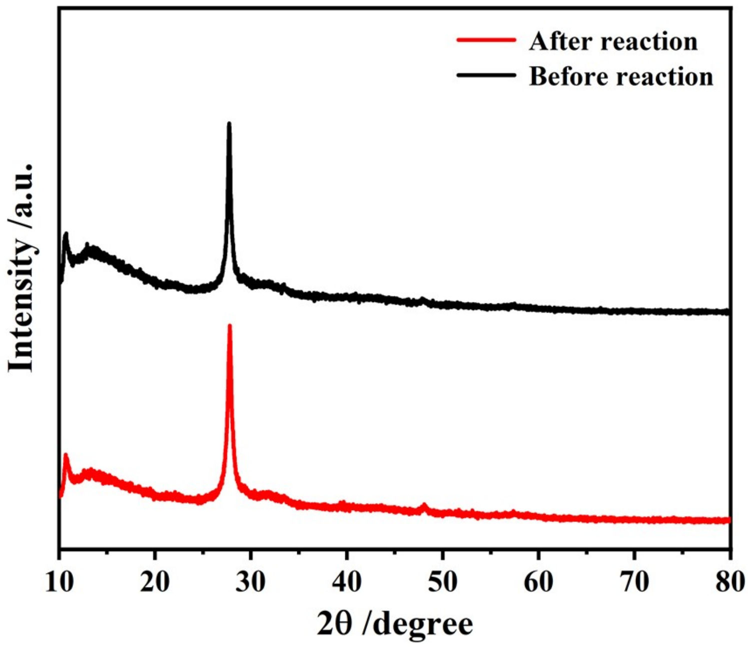

Fig. S3 The XRD patterns of CN/CuS-3 before and after the photocatalytic reaction.

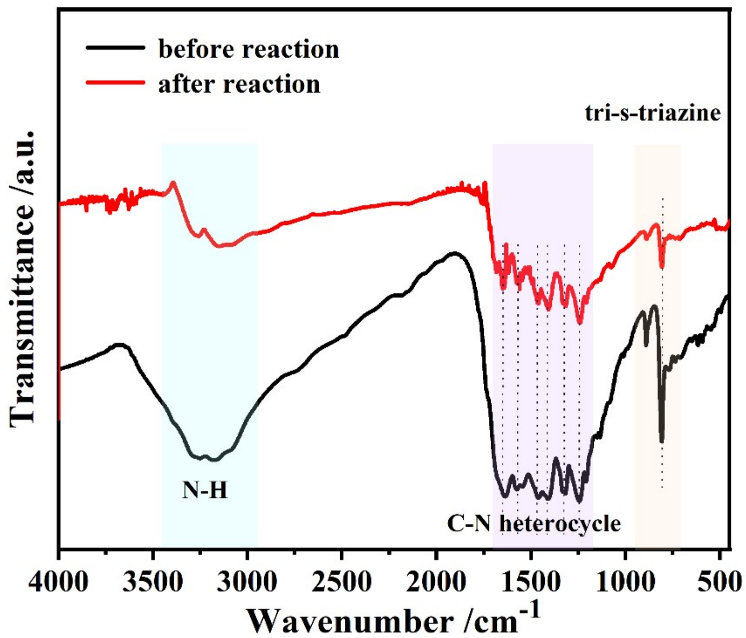

Fig. S4 The FTIR spectra of CN/CuS-3 before and after the photocatalytic reaction.

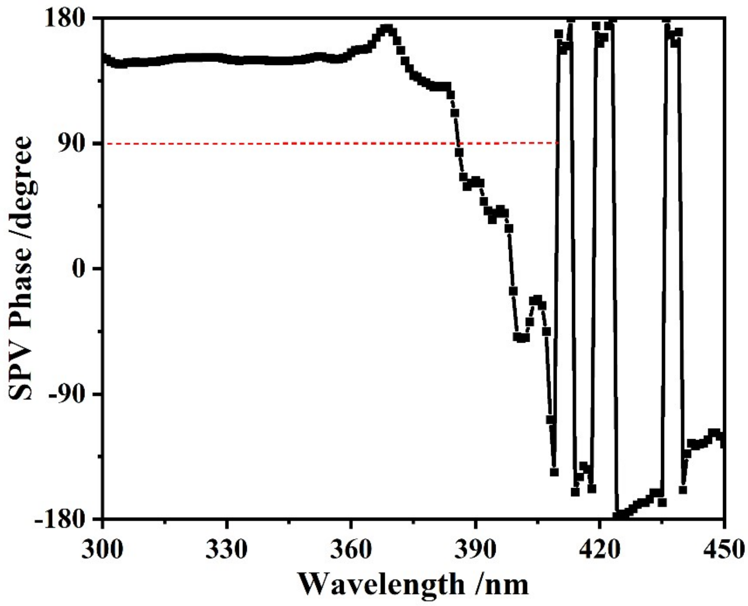

Fig. S5 The SPV spectra corresponding phase spectra of C_3N_4(Li–K).

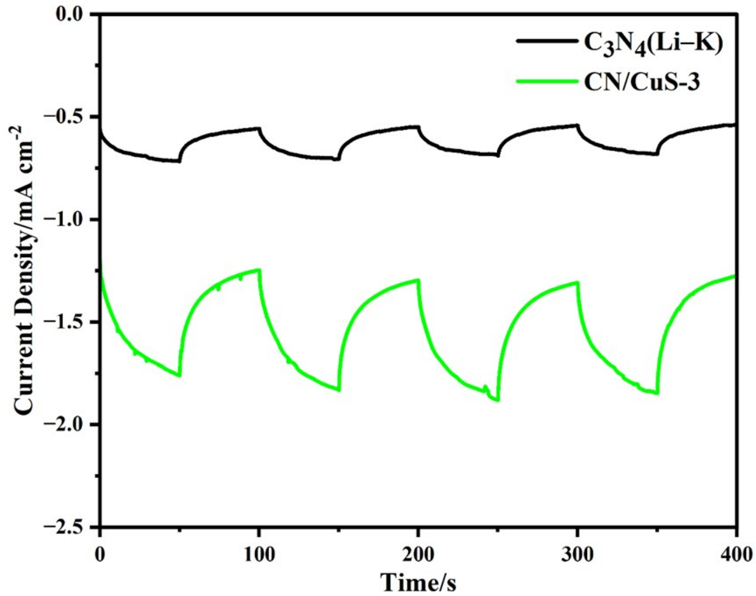

Fig. S6 The transient photocurrent response for C_3N_4(Li–K) and CN/CuS-3 photocatalyst.

Table S1 Salt-assisted carbon nitride-based photocatalysts for hydrogen generation comparison

Photocatalyst	Light Source	Agent	H_2 generation (μmol h^{-1} g^{-1})	Ref (year)
CN/CuS-3		LiCl-KCl	640	This work
3%Pt@HCN	$\lambda > 420$ nm	KCl	392 μmol h^{-1}	(2024)[1]
Pt/g-C_3N_4	$\lambda > 420$ nm	urea	410.51 μmol h^{-1}	(2024)[2]
3%Pt@HTCN-1M H_2SO_4		LiCl-KCl	5764	(2022)[3]

3%Pt@CNHC	λ > 420 nm	NaCl-KCl	6465.4	(2024)[4]
Pt@7.5% H_3BTC/CN		H_3BTC	301	(2021)[5]
Pt@NDCCN	visible light	$NaLiCO_3$	111 μmol h^{-1}	(2019)[6]
3%Pt@SCN(KCl-LiCl)	λ >420 nm	LiCl-KCl	3440.21	(2025)[7]
2%Pt@Cs-CN-2h	λ >420 nm	CsCl	6.17	(2019)[8]

1. C. Wang, Y. H. Lu, Z. Q. Wang, H. W. Liao, W. M. Zhou, Y. H. He, S. M. Osman, M. An, Y. Asakura, Y. Yamauchi, L. W. Wang, Z. H. Yuan. Salt-assisted construction of hydrophilic carbon nitride photocatalysts with abundant water molecular adsorption sites for efficient hydrogen production. Appl. Catal. B: Environ. Energ., 2024, 350, 123902.

2. H. Yang, A. W. Zhang, J. J. Ding, R. Hu, Y. Gong, X, Y, Li, L. Chen, P. Chen, X. Y. Tian. Amino modulation on the surface of graphitic carbon nitride for enhanced photocatalytic hydrogen production. Carbon, 2024, 219, 118841.

3. X. R. Chen, X. Li, J. Wu, C. Fang, J. Ding, H. Wan, G. F. Guan. Boosting photocatalytic H_2 evolution by ingenious construction of isotype heptazine/triazine based porous carbon nitride heterojunction. Sep. Purif. Technol., 2022, 297, 121490.

4. S, L, Wang, F, T, He, Y. M. Lu, Y. Z. Wu, Y. Zhang, P. Dong, X. M. Liu, C. C. Zhao, S. J. Wang, D. J. Wang, J. Q. Zhang, S. B. Wang. Enhancing photocatalytic hydrogen production of carbon nitride: Dominant advantage of crystallinity over mass transfer. J. Colloid Interf. Sci., 2024, 654, 317-326.

5. D. H. Yuan, X. R. Chen, Z. Y. Li, C. Fang, J. Ding, H. Wan, G. F. Guan. The impact of benzene ring embedding on the performance of carbon nitride for photocatalytic hydrogen. Appl. Surf. Sci., 2021, 569, 151089.

6. G.-Y. Zhug, W.-D. Zhang. Boosting photocatalytic hydrogen evolution rate over carbon nitride through tuning its crystallinity and its nitrogen composition. J. Colloid Interf. Sci., 2019, 555, 268-275.

7. R. Y. Han, Y. Z. Wang, Z. Y. Liu, J. S. Wang. Synthesis of crystalline heptazine-based carbon nitride microtubes for highly efficient hydrogen evolution photocatalysis. ACS Appl. Energy Mater., 2025, 8, 2, 883-893.

8. W. M. Xu, X. H. An, Q. G. Zhang, Z. Li, Q. H. Zhang, Z. Yao, X. K. Wang, S. Wang,

J. T. Zheng, J. Zhang, W. T. Wu, M. B. Wu. Cesium salts as mild chemical scissors to trim carbon nitride for photocatalytic H_2 evolution. ACS Sustainable Chem. Eng., 2019, 7, 14, 12351-12357.

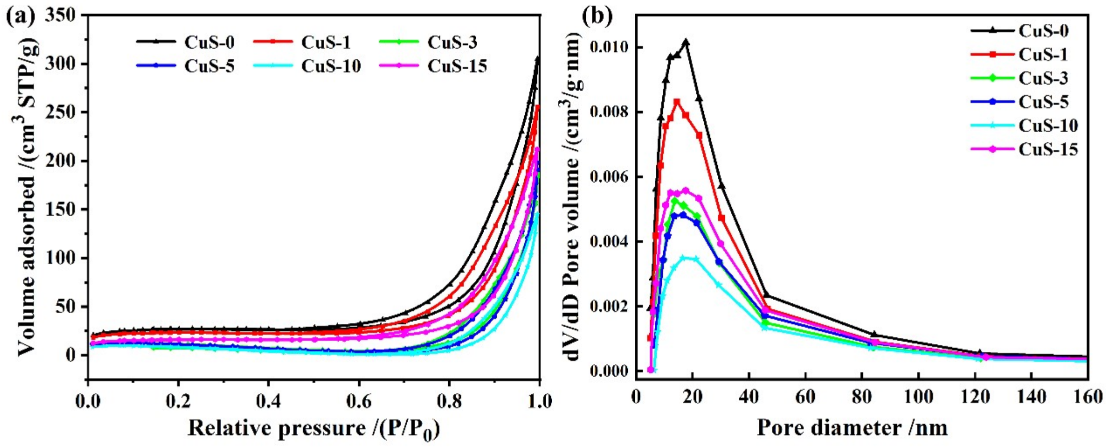

Fig. S7 (a–b) Nitrogen adsorption-desorption isotherms and corresponding pore size distribution of C_3N_4 (Li-K) and CuS/C_3N_4 (Li-K) samples.

Table S2 BET surface area and corresponding pore size of C_3N_4 (Li-K) and CuS/C_3N_4 (Li-K) samples

Thermophysical properties	C_3N_4(Li–K)	CN/CuS-1	CN/CuS-3	CN/CuS-5	CN/CuS-10	CN/CuS-15
S_{BET} ($m^2 \cdot g^{-1}$)	90.3	78.5	34.6	36.4	27.0	55.6
Average pore size (nm)	18.8	18.1	28.2	27.7	28.6	20.8

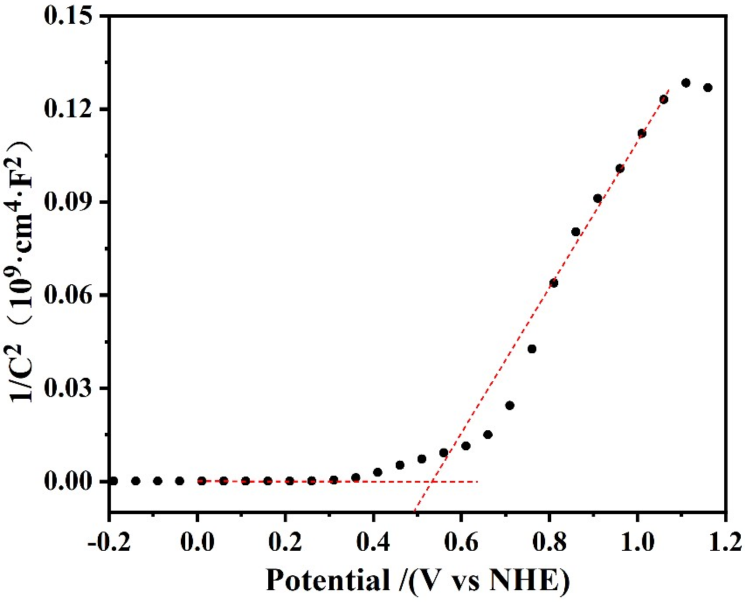

Fig. S8 M-S plots of CuS.